Available online at www.sciencedirect.com
SCIENCE DIRECT®
Biochemical and Biophysical Research Communications 329 (2005) 152–160
BBRC
www.elsevier.com/locate/ybbrc

Solution structure of humanin, a peptide against Alzheimer's disease-related neurotoxicity☆

Dimitra Benaki[a], Christos Zikos[b], Alexandra Evangelou[b], Evangelia Livaniou[b], Metaxia Vlassi[a], Emmanuel Mikros[c,*], Maria Pelecanou[a,*]

[a] *Institute of Biology, NCSR "Demokritos," 153 10 Athens, Greece*
[b] *Institute of Radioisotopes and Radiodiagnostic Products, NCSR "Demokritos," 153 10 Athens, Greece*
[c] *Division of Pharmaceutical Chemistry, University of Athens, Panepistimiopolis, Zografou 157 71, Athens, Greece*

Received 7 January 2005

Abstract

Humanin is a newly identified 24-residue peptide that suppresses neuronal cell death caused by a wide spectrum of familial Alzheimer's disease genes and the β-amyloid peptide. In this study, NMR and circular dichroism studies of synthetic humanin in aqueous and 30% 2,2,2-trifluoroethanol (TFE) solutions are reported. In aqueous solution, humanin exists predominantly in an unstructured conformation in equilibrium with turn-like structures involving residues Gly5 to Leu10 and Glu15 to Leu18, providing indication of nascent helix. In the less polar environment of 30% TFE, humanin readily adopts helical structure with long-range order spanning residues Gly5 to Leu18. Comparative 3D modeling studies and topology predictions are in qualitative agreement with the experimental findings in both environments. Our studies reveal a flexible peptide in aqueous environment, which is free to interact with possible receptors that mediate its action, but may also acquire a helical conformation necessary for specific interactions and/or passage through membranes.

Keywords: Humanin; Alzheimer's disease; Neuroprotection; NMR; CD; Molecular modeling

Alzheimer's disease (AD) is the most prevalent neurodegenerative disease in the ageing population leading to progressive and ultimately fatal loss of mental capacity and it is estimated that 22 million people around the world will be so afflicted by 2025 [1,2]. One of the predominant neuropathological features of the AD brain are the extracellular amyloid deposits in the cerebral and limbic cortices, and in the wall of meningeal and cerebral blood vessels consisting mainly of fibrils of the β-amyloid protein (β-AP) [3]. All genetic and pathological data suggest that β-AP, which is neurotoxic in vitro, plays a central role in the pathway which culminates in neuronal death and dementia [4,5].

The majority of AD cases are of sporadic type, and only 5% of the cases are familial with an autosomal dominant mode of inheritance. Although the cause of sporadic AD is as yet unknown, genetic studies have identified mutations in several genes responsible for the early-onset familial AD (FAD), including the amyloid precursor protein (APP) on chromosome 21, and the homologous presenilin proteins PS1 and PS2 on chromosomes 14 and 1, respectively [6,7]. Expression of FAD mutant APP and PS genes causes neuronal cell death in cultures [8], however little is understood about the intracellular mechanisms for cytotoxicity by the FAD mutant genes.

☆ Humanin structure has been deposited with the RCSB Protein Data Bank, File Name: 1Y32.

* Corresponding authors. Fax: +30210 7274747 (E. Mikros), +30210 6511767 (M. Pelecanou).
E-mail addresses: mikros@pharm.uoa.gr (E. Mikros), pelmar@bio.demokritos.gr (M. Pelecanou).

0006-291X/$ - see front matter © 2005 Elsevier Inc. All rights reserved.
doi:10.1016/j.bbrc.2005.01.100

Recently, Hashimoto et al. [9] identified through functional expression screening, a gene, designated humanin cDNA, encoding a novel 24-residue peptide (H_2N-Met-Ala-Pro-Arg-Gly-Phe-Ser-Cys-Leu-Leu-Leu-Leu-Thr-Ser-Glu-Ile-Asp-Leu-Pro-Val-Lys-Arg-Arg-Ala-COOH) with neuroprotective action against AD-relevant insults. Specifically, humanin suppresses cell death caused by all kinds of the three types of mutant FAD genes, by anti-APP antibody, and by the neurotoxic β-AP in primary neurons, neuronal cell lines, and human cerebrovascular smooth muscle cells [9–12]. Humanin does not affect β-AP production and deposition but directly inhibits the various intracellular downstream toxic mechanisms triggered by FAD mutants or β-AP. The neuroprotective properties of humanin are specific for FAD mutations and β-AP toxicity because humanin is not effective in protecting neurons against the toxic fragments of the prion protein [12], or the overexpression of polyQ mutants associated with Huntingtons's disease and spinocerebellar ataxia [9]. The efficacy and selectivity of humanin's action against a very wide spectrum of AD insults suggest that humanin may serve as a probe in the development of a new mode of AD therapy aiming at neuroprotection.

The auspicious properties of humanin, combined with the fact that extensive structure/function studies have linked its neuroprotective action to its primary sequence [13–15], prompted us to investigate its solution structure with NMR and circular dichroism (CD) spectroscopies, structure calculations, and comparative 3D modeling.

Materials and methods

Preparation of humanin. Humanin was prepared by Fmoc-solid phase synthesis [16] on an in-house prepared *o*-Cl-trityl-amidomethyl polystyrene resin. The peptide was purified to 95% with semi-preparative RP-HPLC and suitably characterized.

CD spectropolarimetry. CD spectra of humanin in the range 250–180 nm were recorded on a Jasco J715 spectropolarimeter using 1 mm quartz cells, 1 nm bandwidth, 0.2 nm resolution, 1 s response, and an average of 8 scans for each spectrum. The temperature of the samples was regulated with a Peltier temperature control system. The concentration of humanin in most runs was 0.19 mg/mL (0.07 mM). The effect of humanin concentration on the CD spectra was studied in solutions ranging from 4.5 to 0.045 mg/mL (1.7–0.017 mM). Samples in TFE were prepared by adding the proper amount of a 4.5 mg/mL stock solution to water/TFE mixtures to achieve the desired humanin concentration. The pH of the aqueous solutions of humanin was around 2.7 while the pH of the water/TFE mixtures ranged from 2.7 to 3.2 (uncorrected for the presence of TFE).

The CD spectra were analyzed with the CDNN program [17] which uses precompiled neural networks for the deconvolution of the spectra.

NMR spectroscopy. Aqueous solution studies of humanin at pH 2.7 and 5.5 were undertaken in H_2O/D_2O 9:1 containing 60 μM NaN_3 to prevent microbial growth. The concentration of humanin in the NMR samples was 1.7 mM. The effect of humanin concentration on the NMR spectra was studied in solutions ranging from 3.6 to 0.3 mM. The pH was adjusted by the addition of DCl and NaOD solutions. TFE studies were carried out in H_2O/TFE-d_3 7:3 solutions at pH 2.8 (uncorrected for the presence of TFE).

NMR spectra were obtained on a Bruker Avance DRX 500 MHz spectrometer. Typically, spectra were recorded with sweep width of 12 ppm, 2048 data points, 400 t1 increments, and 1.5 s relaxation delay between cycles. Mixing times of 100, 150, and 200 ms were used for the NOESY spectra. The MLEV-17 spin lock sequence with mixing time of 80 ms was used for the TOCSY spectra. Water peak suppression was performed with the excitation sculpting pulse sequence. Spectra were referenced to internal DSS.

The temperature dependence of the amide signals was followed through a series of TOCSY spectra recorded at six different temperatures (2, 7, 12, 19, 25, and 32 °C).

All NMR spectra were processed using XWIN-NMR version 2.6 and were analyzed on PC using the Sparky program (T.D. Goddard, D.G. Kneller, SPARKY 3).

Structure calculations. Interproton distance restraints were derived through volume integration of the NOESY cross-peaks (mixing time 150 ms, 7 °C) using the Sparky software. Peak intensities of known distance (1.79 Å for the distance between two hydrogens of methylene) were used for calibration. The consistency of this calibration was verified on other geminal proton distances. Lower distance bounds were taken as the sum of the van der Waals radii of 1.8 Å.

Starting from an extended structure, structural calculations were performed using the simulated annealing and energy minimization protocol in the program CNS, version 1.1 [18]. The procedure included a constant high-temperature (5000 K) torsion-angle annealing protocol, a slow cooling stage with torsion-angle dynamics, and 5000 steps of restraint Powell energy minimization. In the first stage of structure calculation, only unambiguously assigned nOe distance restraints were used. In the following stage, hydrogen bonds were included as restraints for regular secondary structure elements, since their existence is detected in the preliminary nOe based structures and is corroborated by the low temperature coefficient values.

A total of 300 accepted structures with no distance violation larger than 0.2 Å were generated. From these structures, the 14 convergent structures were selected having the lowest energy, the best structural quality in Ramachandran plot, and the lowest mutual RMS deviation. The covalent geometry of the conformers generated was analyzed using PROCHECK [19]. Maestro 6.5 Schrödinger Inc Software was used for the superposition of the generated structures.

3D-modeling. Secondary structure predictions were performed using the Network Protein Sequence Analysis (NPS) web-server [20]. The humanin sequence was used as query in sequence similarity searches against the Protein Data Bank database [21] in order to identify protein domains of known three-dimensional structure that share high percent sequence identity with the humanin peptide. The Gapped BLAST and PSI-BLAST programs [22] of the NCBI web server were used for this purpose. Coordinates from the 2.2 Å crystal structure of *Salmonella* tyrosine phosphatase SPTP (PDB entry: 1G4W) [23] were used as template for the modeling of the structure of the humanin Phe6-Leu18 region. The 3D modeling was performed using the Swiss-PdbViewer v3.7b2 program [24]. The initial model was subsequently subjected to energy minimization in vacuo using a version of GROMOS force field [25] as implemented in Swiss-PdbViewer v3.7b2. The quality of the final models was assessed with the PROCHECK suite of programs [19].

Results

CD study

The CD spectra of humanin (0.19 mg/mL, 0.07 mM) in aqueous solutions in the presence of various concentrations of TFE at 25 °C are shown in Fig. 1A. In the absence of TFE, the CD spectrum shows strong negative

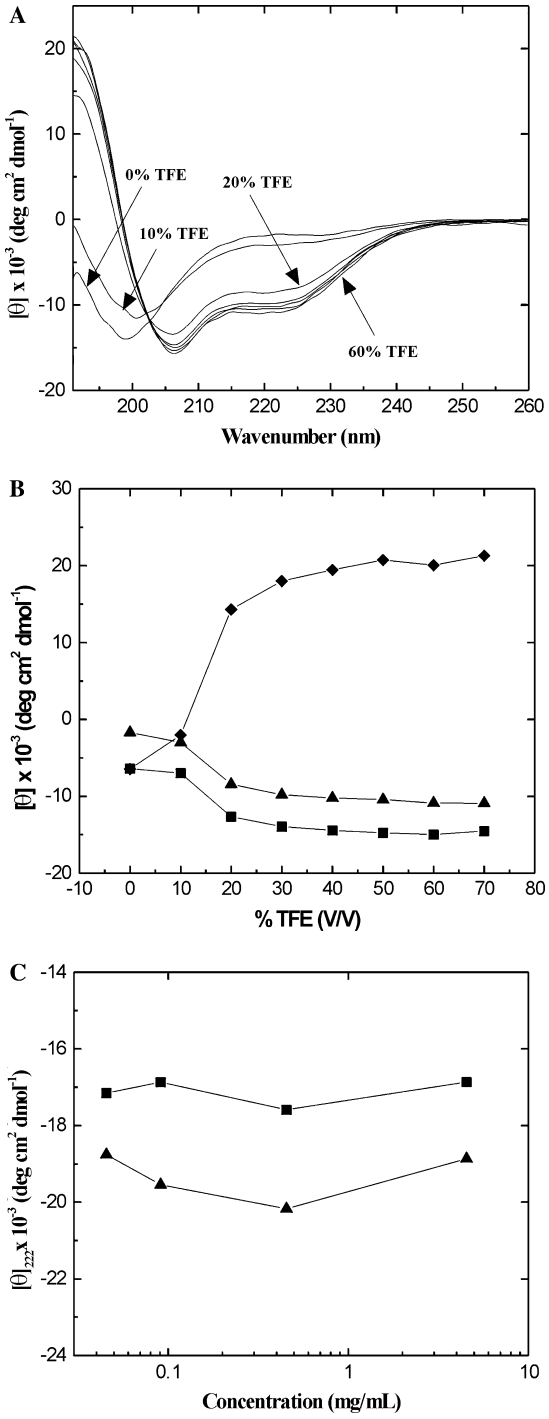

Fig. 1. (A) CD spectra of humanin in different TFE/H_2O solutions, ranging from 0% to 60% by intervals of 10%, at 7 °C. (B) Dependence on TFE concentration of the ellipticity at 192 [♦], 208 [■], and 222 nm [▲] of humanin at 7 °C. (C) Concentration dependence of the mean residue ellipticity at 222 nm of a 30% TFE solution at 7 °C [▲] and 25 °C [■]. The peptide concentration is on a log scale. The lower $[\theta]_{222}$ value at 7 °C compared to 25 °C is apparently due to an increase in the population of helical conformers.

dichroism below 200 nm, indicative of a small degree of ordering in the peptide [26]. On addition of TFE, changes diagnostic of conformational equilibrium between unordered structures and helical conformations of humanin in solution take place in the CD spectra [27]. The mean residue ellipticity values $[\theta]$ recorded at 192, 208, and 222 nm with increasing v/v% of TFE are graphically depicted in Fig. 1B and are characteristic of the presence of increasing helix populations in solution [28,29]. The maximum helical content was recorded at 30% TFE above which no significant changes were observed in the shape of the CD curves. The fact that the maximum helical content of humanin is reached at the relatively low TFE concentration of 30% indicates a pronounced helical propensity for the peptide [30]. Deconvolution of the CD spectra with the CDNN program gave a helical content of 6% in the absence of TFE and 33% in the presence of 30% TFE.

Concentration dependence CD studies were carried out in aqueous solution and in the presence of 30% TFE (Fig. 1C) with sample concentrations differing by two orders of magnitude from 4.5 to 0.045 mg/mL (1.7–0.017 mM). The value of $[\theta]_{222}$ remained relatively constant at the different concentrations, ruling out the possibility of self-association.

NMR structural study in aqueous solution

Aqueous solution NMR studies were carried out at 25 and 7 °C, at humanin concentration of 1.7 mM, and pH 2.7 and 5.5. Acidic conditions were chosen because amide hydrogen exchange is sufficiently low to allow the observation of the amide protons under the solvent suppression conditions. In addition, oxidation of cysteines and formation of disulfide bridges between cysteine residues are promoted in basic pH [31]. A concern over performing the structure determination at a non-physiological pH was addressed in part by the CD studies where no major differences were recorded in the CD spectra between pH 2.7 and 6.9 (data not shown).

The NMR spectra showed that the sample was of high purity. No deterioration of the sample or loss of signal was detected over time under the conditions employed.

All amino acids were assigned through the combined use of TOCSY and NOESY spectra according to the standard sequential assignment procedure [32]. The ^1H resonance assignments at 25 °C, and pH 2.7 and 5.5 are given in the Supplementary material (Tables S1 and S2, respectively). Chemical shift changes >0.1 ppm in relation to pH were only observed for the C-terminal Ala24 as well as for the Glu15 and Asp17 residues, the pK_as of which (4.25 and 3.86, respectively) lie within this pH range. Both Pro3 and Pro19 residues were found to be in the trans configuration.

Fig. 2A shows the chemical shift indices [33,34] for the αCH protons of all amino acid residues of humanin at 25 °C and pH 2.7. As it is obvious from the graph,

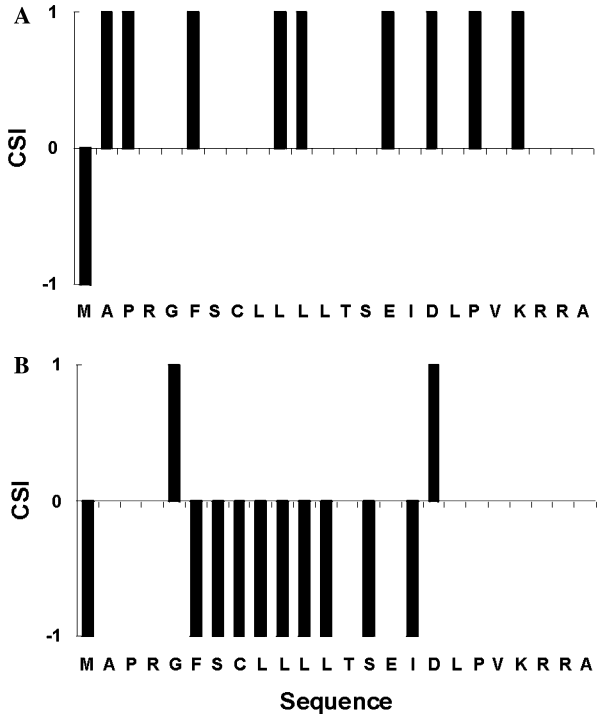

Fig. 2. Chemical shift indices for the αCH protons of humanin in aqueous solution at pH 2.7 (A) and in 30% TFE solution (B) at 25 °C. The Wishart values for random coil shifts were used [34].

neither consecutive "−1's," indicative of α-helix, nor consecutive "1's," indicative of β-strand, are present and the structure is best described as coil, a term which incorporates loops, random coils, turns, etc. Similar results were obtained at pH 5.5.

NOESY spectra were recorded at 7 °C where connectivities are clearly identified since both the correlation time of the molecule and the mole fraction of stabilized conformers are likely to be increased. The intraresidue $d_{\alpha N}(i,i)$, sequential $d_{\alpha N}(i,i+1)$, $d_{NN}(i,i+1)$, and medium range $d_{\alpha N}(i,i+2)$ nOes for humanin at pH 2.7 are shown in Fig. 3A. In agreement with the CD data, the presence of relatively strong, sequential $d_{\alpha N}(i,i+1)$ connectivities over the whole sequence of humanin indicates that the conformational ensemble of the peptide includes a substantial population of extended chain forms [28,29]. The presence however, of weak but definite $d_{NN}(i,i+1)$ and $d_{\alpha N}(i,i+2)$ connectivities extending over the range of 17 residues from Gly5 to Lys21 provides evidence for the existence of turn loci between these amino acids and the presence of folded conformations in equilibrium with the extended. The most intense $d_{NN}(i,i+1)$ connectivities are observed in the region between Glu15 and Leu18, indicating that the highest population of the structured conformers occur in this region in the aqueous environment. Furthermore, the presence of medium-range nOe connectivities between the aromatic ring protons of Phe6 and the β, γ, and δ protons of the side chains of Leu9 and/or Leu10, in addition to $d_{NN}(i,i+1)$ and $d_{\alpha N}(i,i+2)$ connectivities between residues Gly5 to Leu9, provides further evidence for a local turn conformation in this part of the sequence, stabilized by hydrophobic interactions between side chains of

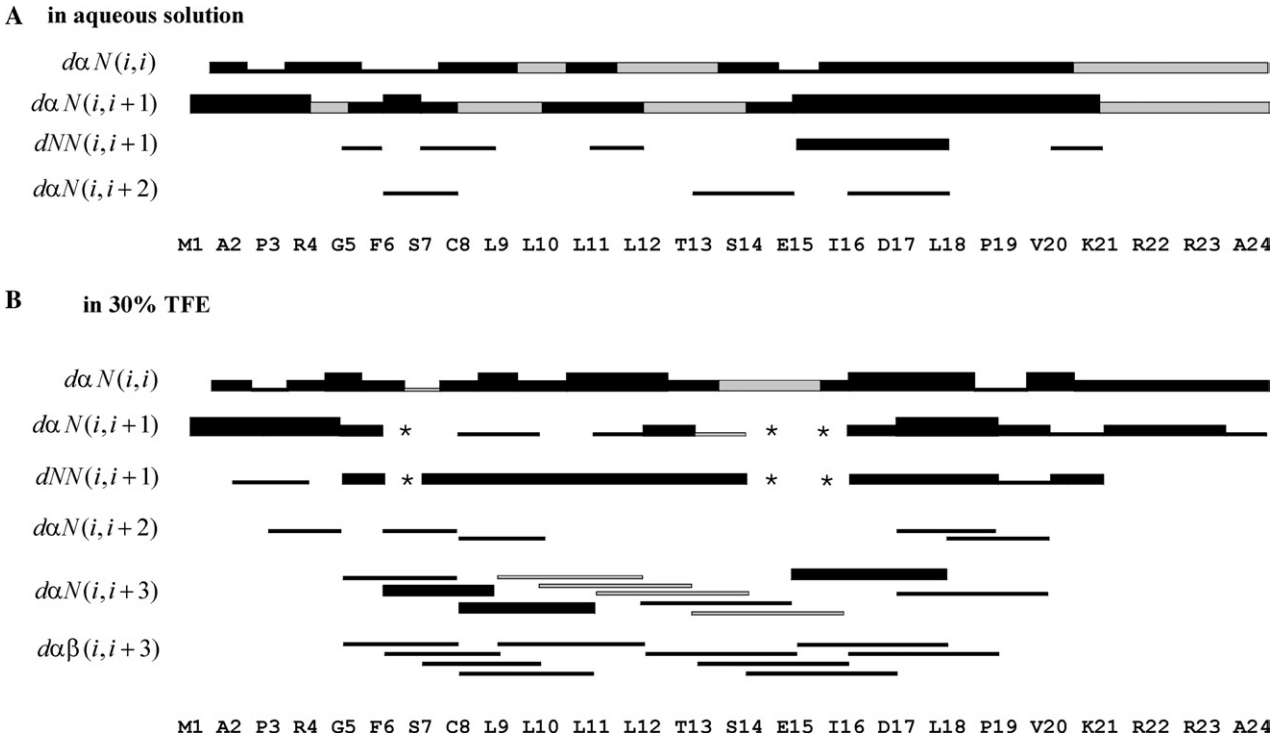

Fig. 3. Schematic representation showing the relative intensity (filled bars) of the nOe connectivities in aqueous (A) and in 30% TFE (B) solutions. Gray bars represent nOes of ambiguous intensity, while asterisks refer to nOes that cannot be detected due to severe overlap.

phenylalanine and leucines [35]. The nOe cross-peaks between Phe6 and Leu9/Leu10 cannot be attributed to spin diffusion as they are observed even in the spectra with the shortest mixing time of 100 ms.

The possibility of existence of ionic interactions between the side chains of Glu15 or Asp17 and the side chain of Lys21 is rather excluded at pH 2.7 where both side chains are expected to be in their undissociated forms. At the experiments conducted at pH 5.5, where the acidic residues are ionized and ions of opposite charge exist in solution, no changes were observed in the NOESY spectra, indicating that ionic attraction does not contribute to the stabilization of the conformation of humanin under the specific conditions [36].

The temperature dependence of the amide proton chemical shifts of humanin in aqueous solution was determined over the range 2–32 °C. For all amide protons, the chemical shift varied linearly with temperature, suggesting that no major conformational rearrangements occur in the temperature range employed, a fact which is confirmed by the CD thermal studies. The temperature coefficients [37] for each amino acid residue are incorporated in Tables S1 and S2 of the Supplementary material. Their average value of 7.0 ± 1.1 ppb/°C at pH 2.7, and 7.3 ± 1.3 ppb/°C at pH 5.5 is in agreement with the existence of a low population of ordered states in aqueous solution.

In agreement with the CD concentration studies, no changes in chemical shifts or linewidths were observed over a 12-fold dilution of the sample (concentrations ranging from 3.6 to 0.3 mM). This fact indicates that aggregates are not present in the samples studied and that the nOe patterns observed are not induced by an intermolecular association.

NMR structural study in 30% TFE

NMR studies of humanin were also conducted in the presence of 30% TFE which, according to the CD data, is the minimum percentage of TFE that is sufficient for the peptide to assume its maximum helicity. The NH to aliphatic proton region of the TOCSY spectrum (Fig. S1), and the backbone amide region of the NOESY spectrum (Fig. S2) along with the ^{1}H resonance assignments (Table S3) are provided as Supplementary material. As it is obvious from Fig. 3B, which summarizes the nOe connectivities observed, in 30% TFE a large number of sequential and medium-range connectivities, characteristic of the presence of helical structure populations [29], are clearly identified. These include the relatively strong sequential $d_{NN}(i,i+1)$ connectivities between residues Gly5 to Lys21, and the nearly complete sets of $d_{\alpha N}(i,i+3)$ and $d_{\alpha\beta}(i,i+3)$ connectivities between residues Gly5 to Val20 and Gly5 to Pro19, respectively.

Additional evidence that the peptide adopts partially helical structure is provided by the upfield shift of the αCH resonances compared to the random coil values [34,38] generating a series of "−1" chemical shift indices in the region spanning 11 residues from Phe6 to Ile16. This dense grouping of "−1"s, which exceeds 70%, identifies a helix. The fact that $d_{\alpha N}(i,i+2)$ connectivities of comparable intensity to the $d_{\alpha N}(i,i+3)$ and $d_{\alpha\beta}(i,i+3)$ connectivities are recorded among residues that participate in the helical conformation indicates that helical conformations exist in solution in equilibrium with other turn-like structures.

The chemical shift index analysis indicates termination point for the helix at Asp17 which is the first amino acid with a chemical shift index opposite in sign to that of the helical structure [33]. The fact that $d_{\alpha N}(i,i+3)$ and $d_{\alpha\beta}(i,i+3)$ connectivities are observed in the Glu15–Pro19 region of the sequence may indicate helix fraying at this part of the peptide or a turn-like structure, a fact which is supported by the presence of a proline residue at position 19.

The temperature coefficients for each amino acid residue in 30% TFE are reported in Table S3 of the Supplementary Material section. Values of temperature coefficients <3 ppb/°C indicative of the involvement of the amide proton in intramolecular hydrogen bonding are observed for residues Ser7 to Leu10. The rest of the coefficients show a mean value of 5.4 ppb/°C (±1.8 ppb/°C) indicative of the existence of ordered structures.

Structural calculations were performed using the simulated annealing protocol implemented in the CNS solve 1.1 [18]. Starting from an extended structure, a total of 300 accepted structures with no distance violation larger than 0.2 Å were calculated. The 60 lowest energy structures had relative energies of up to 5 kcal/mol compared to the global minimum. Fourteen out of the 60 structures exhibiting the lowest energy, the best structural quality in Ramachandran plot, and the lowest mutual RMS deviation were selected for further analysis using PROCHECK [19]. The statistical data for the calculation are summarized in Table 1. The distribution of all the residues in the Ramachandran plot indicates the overall quality: 73.3% of the residues are in the most favorable region and 20.7% in the general region. No violations of nOe restrains greater than 0.1 Å were observed. The backbone of the 14 structures could be defined with an RMS deviation value of 0.95 (±0.23) Å for residues 4–18 and their superposition is shown in Fig. 4. The generated structures reveal the existence of a well-defined helical part spanning residues Gly5 to Asp17 and confirm that the nOe distance restraints are consistent with a helix in this region. These results are well in agreement with all the CD and NMR spectral data already presented.

3D-Model of humanin

As indicated by the sequence similarity searches, a 13 amino acid region of humanin peptide (aa: 6–18) shares

Table 1
NMR-derived restraints and structural statistics for the 14 final lowest energy structures of humanin

Experimental restraints	
Intraresidue nOes	50
Sequential nOes	64
Medium range nOes ($i,i+2$; $i,i+3$; $i,i+4$)	75
Hydrogen bonds (H–O distances)	5
Total	194
RMSD from experimental data	
Distances (Å)	0.026 ± 0.002
Coordinate precision (Å, mean pairwise)	
RMSD (Å) of residues 4–18, backbone atoms	0.95 ± 0.23
CNS final energies (kcallmol)	
E_{total}	35.25 ± 0.65
E_{bond}	1.74 ± 0.19
E_{angle}	18.87 ± 0.29
E_{improp}	0.76 ± 0.13
E_{vdw}	4.35 ± 0.31
E_{nOe}	9.53 ± 0.50
RMSD from idealized covalent geometry	
Bond lengths (Å)	0.0017
Bond angles (°)	0.349
Ramachandran analysis from PROCHECK-NMR (%)	
Most favored regions	73.31
Additionally allowed regions	20.69
Generously allowed regions	4.51
Disallowed regions	1.51

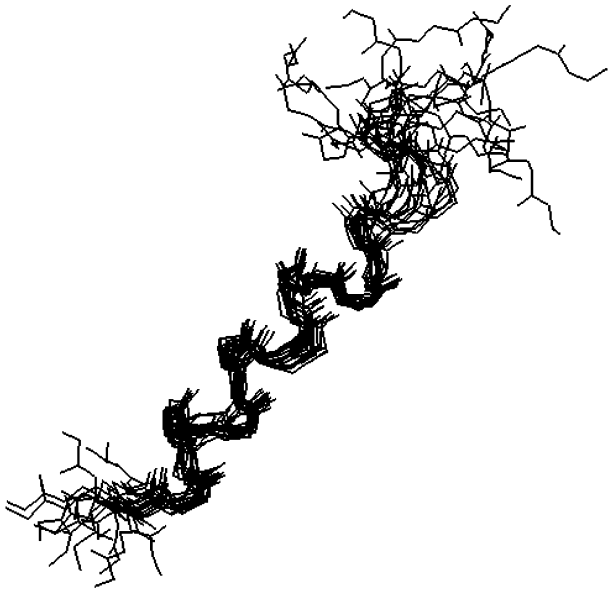

Fig. 4. Superposition of the backbone (N, αC, and C) atoms of the 14 best structures obtained from CNS simulated annealing calculations. The structures are fitted to the helical region residues 4–18.

a high sequence similarity (53.8% identity and 84.6% similarity) with a domain (aa: 209–221) of *Salmonella* tyrosine phosphatase and GTPase activating protein SPTP, the crystal structure of which has been determined at 2.2 Å (PDB entry: 1G4W) [23]. The coordinates from the 1G4W entry corresponding to SPTP (209–221) region were used as a template for the modeling of the humanin (6–18) three-dimensional structure and the proposed model is shown in Fig. 5. According to the model, there is a bend (of approximately 45°) of the polypeptide chain around residue Ser7. This backbone bending results in a close contact between the side chains of Phe6 and Leu9, in agreement with the NMR data in aqueous solution where interactions between Phe6 and Leu9/Leu10 are detected. A second turn of the polypeptide chain involves residues Ser14 to Leu18 which is also in agreement with the NMR observations. The region between the two bends has a rather extended conformation with the ϕ, ψ conformational angles of Cys8, Leu9, Leu10, and Leu11 lying in the β-strand region of the Ramachandran plot. The tendency of these residues to adopt an extended β-strand conformation has been also suggested by secondary structure predictions (Supplementary material, Fig. S3). The β-strand region of the humanin peptide could be involved in interactions with β-strands of other proteins and β-sheet formation or in self-interactions between humanin molecules.

Since, as shown by NMR experiments, humanin adopts an α-helical conformation in the less polar environment of 30% TFE, its propensity for transmembrane helix formation was checked. Several transmembrane prediction web-servers were used for this purpose with the humanin sequence as query. Among them the Dense Alignment Surface method (DAS) [39] predicted a potential transmembrane segment of 11 amino acids starting from Gly5 (with a hit of 1.7). This is in agreement with the NMR experiments suggesting that the humanin (5–15) region has a potential to adopt an α-helical conformation in hydrophobic environments.

Discussion

The potent in vitro neuroprotective activity of humanin against the insults of the AD-related genes and the neurotoxic β-amyloid peptide has spurred new hopes for the development of a pharmaceutical therapy against AD. To establish therapeutic strategies, as well as to clarify the mechanism of AD pathogenesis, the mode of humanin action must be understood. Our CD, NMR, and 3D comparative modeling data demonstrate that in aqueous solution humanin possesses essentially no stable secondary structure, but interconverts between turn-like conformations in which the regions Gly5-Leu9 and Glu15-Leu18 appear to be the more ordered. This ensemble of secondary structures can be characterized as nascent helix [28] since it is readily stabilized in an ordered helical conformation in the less polar environment of 30% aqueous TFE. The relatively low TFE concentration of 30% required for humanin to acquire its

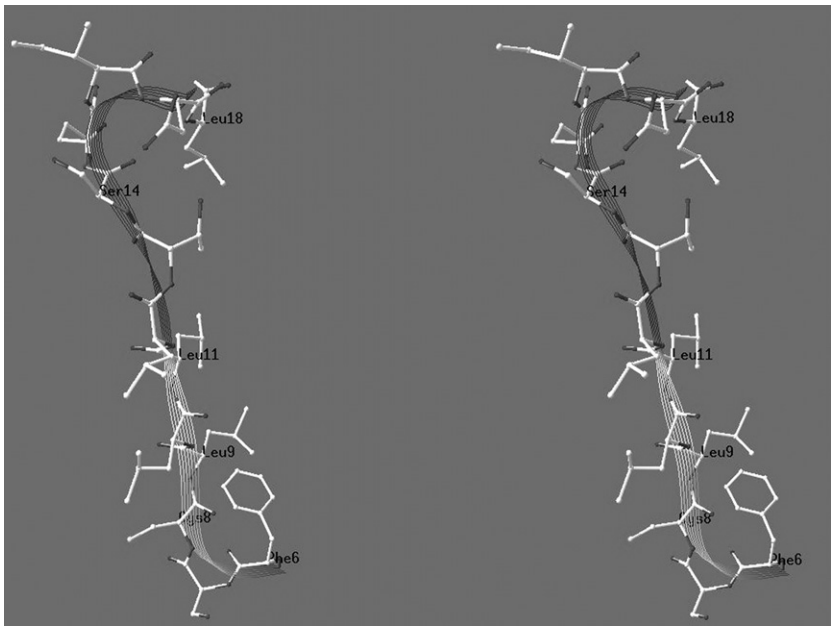

Fig. 5. Stereo-view of the three-dimensional model of humanin (6–18) peptide. The ribbon representation is used to depict the αC tracing of the polypeptide chain. A kink of the polypeptide chain near the N-terminus results in a close contact between the side chains of Phe6 and Leu9, whereas a second bend close to the C-terminus involves residues Ser14-Leu18. Both predictions are in agreement with the NMR observations in aqueous solution. The region between Cys8 and Leu11 is predicted to adopt an extended conformation with the ϕ, ψ conformational angles in the β-region of the Ramachandran plot in accordance with secondary structure predictions.

maximum helical content indicates a pronounced helical propensity for the peptide [30]. It is thus possible that in the cell, immediately after synthesis, humanin exists predominantly in an unstructured conformation in equilibrium with turn-like structures, but may acquire helical conformation when found in the more lipophilic environment of membranes.

The variation in secondary structure of humanin according to the environment may play an important role in the process of its extracellular secretion. It has been shown [9,13,14] that in order to exert cytoprotection, humanin must be secreted into the cultured medium, a fact that indicates that humanin acts only from outside of the cell. Furthermore, the existence of a specific receptor mediating the action of humanin has been demonstrated by the existence of specific binding of the radiolabeled humanin variant, S14G, on the cell surface [9], while humanin and humanin-related peptides have been recently reported to act as specific ligands for formyl peptide receptor-like 1 and 2 [40]. The complex process of secretion involves interactions with the lipid bilayer of the endoplasmic reticulum (ER) membrane, as well as interactions with molecular chaperones and processing enzymes present in the ER lumen [41]. The ability of humanin to acquire helical conformation may facilitate the passage through the lipophilic environment [42] of the ER membrane, while its flexibility in the cytosolic milieu may allow interactions with ER lumen proteins. Construction of Arg-scanned humanin mutants has demonstrated that substitution of Leu9, Leu10, and Leu11 by Arg results in secretion defective mutants, consistent with the functional role of the Leu9–Leu12 region as a hydrophobic core. In this region, the Leu10 residue appears to play a central role because it cannot be substituted by either a basic or acidic residue [14]. This is consistent with the NMR data demonstrating that in the aqueous environment Leu9 and/or Leu10 are in proximity to the aromatic ring of Phe6, a hydrophobic interaction that would be disrupted by substitution of Leu10 by either a basic or a acidic residue.

The amino acid sequence of humanin, which includes a positively charged N-terminal domain, a central hydrophobic region, and a more polar C-terminal domain, conforms to the general design of signal peptides [43]. Humanin has been shown to function as a signal peptide in the case of cells transfected with plasmid encoding enhanced green fluorescent protein (EGFP) fused with humanin [14]. Signal peptides are essential for directing proteins from the cytosol to membrane translocation sites where signal sequences are recognized by membrane-bound translocase proteins with almost 100% selectivity and specificity. Recognition requires the formation of specific secondary structures in the core region of the signal peptide. A possible role for humanin as signal peptide is therefore consistent with its ability to acquire a helical conformation in hydrophobic environments as observed in the present study.

Ala-scanning experiments of the Pro3–Pro19 region of humanin reveal that Pro3, Cys8, Leu9, Leu12,

Thr13, Ser14, and Pro19 are essential residues for neuroprotection [11]. Since substitution of these residues by the apolar amino acid alanine is not expected to affect the conformation of humanin in both aqueous and hydrophobic environments, it appears likely that the differentiation in neuroprotective function in these mutants is due to disruption of necessary interactions of humanin with molecules mediating its action. On the other hand, the enhancement of neuroprotective activity of humanin when Ser14 is substituted by glycine [9,11] may be due to an increase in the conformational flexibility of humanin and the facilitation of interactions with functional counterparts.

Overall, our studies reveal a flexible peptide with definite turn points in its structure that is free to interact with possible receptors that mediate its action, but may also acquire a helical conformation necessary for specific interactions and/or passage through membranes. The peptide is stable in the aqueous environment under the conditions employed, and during the course of the study no aggregation or precipitation from solution was observed. The high potency of the displayed neuroprotection and the specificity for AD-relevant insults suggest that humanin is an appropriate starting point for the investigation of the neurodegeneration mechanism in AD and the development of a curative therapy against it.

Acknowledgments

M. Pelecanou wishes to acknowledge financial support by the National Bank of Greece and C. Zikos wishes to acknowledge a financial grant offered by Biomedica Life Sciences S.A.

Appendix A. Supplementary material

Supplementary data associated with this article can be found, in the online version, at doi:10.1016/j.bbrc.2005.01.100.

References

[1] M.S. Wolfe, Therapeutic strategies for Alzheimer's disease, Nat. Rev., Drug Discov. 1 (2002) 859–866.
[2] J.T. Coyle, D.L. Price, M.R. DeLong, Alzheimer's disease: A disorder of cortical cholinergic innervation, Science 219 (1983) 1184–1190.
[3] G.G. Glenner, Alzheimer's disease: Its proteins and genes, Cell 52 (1988) 307–308.
[4] J.A. Hardy, G.A. Higgins, Alzheimer's disease: The amyloid cascade hypothesis, Science 256 (1992) 184–185.
[5] B.A. Yankner, Mechanism of neuronal degeneration in Alzheimer's disease, Neuron 16 (1996) 921–932.
[6] D. Blacker, R.E. Tanzi, The genetics of Alzheimer disease, Arch. Neurol. 55 (1998) 294–296.
[7] B.S. Shastry, F.J. Giblin, Genes and susceptible loci of Alzheimer's disease, Brain Res. Bull. 48 (1999) 121–127.
[8] I. Nishimoto, A new paradigm for neurotoxicity by FAD mutants of β APP: A signalling abnormality, Neurobiol. Aging 19 (1998) S33–S38.
[9] Y. Hashimoto, T. Niikura, H. Tajima, T. Yasukawa, H. Sudo, Y. Ito, Y. Kita, M. Kawasumi, K. Kouyama, M. Doyu, G. Sobue, T. Koide, S. Tsuji, J. Lang, K. Kurokawa, I. Nishimoto, A rescue factor abolishing neuronal cell death by a wide spectrum of familial Alzheimer's disease genes and Aβ, Proc. Natl. Acad. Sci. USA 98 (2001) 6336–6341.
[10] Y. Hashimoto, Y. Ito, T. Niikura, Z. Shao, M. Hata, F. Oyama, I. Nishimoto, Mechanisms of neuroprotection by novel rescue factor Humanin from Swedish mutant amyloid precursor protein, Biochem. Biophys. Res. Commun. 283 (2001) 460–468.
[11] Y. Hashimoto, T. Niikura, Y. Ito, H. Sudo, M. Hata, E. Arakawa, Detailed characterization of neuroprotection by a rescue factor Humanin against various Alzheimer's disease relevant insults, J. Neurosci. 21 (2001) 9235–9245.
[12] S.S. Jung, W.E. Van Nostrand, Humanin rescues human cerebrovascular smooth muscle cells from Aβ-induced toxicity, J. Neurochem. 84 (2003) 266–272.
[13] T. Niikura, Y. Hashimoto, H. Tajima, I. Nishimoto, Death and survival of neuronal cells exposed to Alzheimer' s insults, J. Neurosci. Res. 70 (2002) 380–391.
[14] Y. Yamagishi, Y. Hashimoto, T. Niikura, I. Nishimoto, Identification of essential amino acids in Humanin, a neuroprotective factor against Alzheimer's disease-relevant insults, Peptides 24 (2003) 585–595.
[15] K. Terashita, Y. Hashimoto, T. Niikura, H. Tajima, Y. Yamagishi, M. Ishizaka, M. Kawasumi, T. Chiba, K. Kanekura, M. Yamada, M. Nawa, Y. Kita, S. Aiso, I. Nishimoto, Two serine residues distinctly regulate the rescue function of Humanin, an inhibiting factor of Alzheimer's disease-related neurotoxicity: Functional potentiation by isomerization and dimerization, J. Neurochem. 85 (2003) 1521–1538.
[16] A. Evangelou, C. Zikos, E. Livaniou, G.P. Evangelatos, High-yield, solid-phase synthesis of humanin, an Alzheimer's disease associated, novel 24-mer peptide which contains a difficult sequence, J. Peptide Sci. 10 (2004) 631–635.
[17] G. Böhm, R. Muhr, R. Jaenicke, Quantitative analysis of protein far UV circular dichroism spectra by neural networks, Protein Eng. 5 (1992) 191–195.
[18] A.T. Brunger, P.D. Adams, G.M. Clore, W.L. Delano, P. Gros, R.W. Grosse-Kunstleve, J.-S. Jiang, J. Kuszewski, M. Nilges, N.S. Pannu, R.J. Read, L.M. Rice, T. Simonson, G.L. Warren, Crystallography and NMR system (CNS): A new software system for macromolecular structure determination, Acta Cryst. D 54 (1998) 905–921.
[19] R.A. Laskowski, M.W. MacArthur, D.S. Moss, P.E. Wright, PROCHECK: A program to check the stereochemical quality of protein structures, J. Appl. Crystallogr. 26 (1993) 283–291.
[20] C. Combet, C. Blanchet, C. Geourjon, G. Deleage, NPS@: Network protein sequence analysis, TIB 25 (2000) 147–150.
[21] H.M. Berman, J. Westbrook, Z. Feng, G. Gilliland, T.N. Bhat, H. Weissig, I.N. Shindyalov, P.E. Bourne, The Protein Data Bank, Nucleic Acids Res. 28 (2000) 235–242.
[22] S.F. Altschul, T.L. Madden, A.A. Schäffer, J. Zhang, Z. Zhang, W. Miller, D.J. Lipman, Gapped BLAST and PSI-BLAST: A new generation of protein database search programs, Nucleic Acids Res. 25 (1997) 3389–3402.
[23] C.E. Stebbins, J.E. Gallan, Modulation of host signalling by a bacterial mimic structure of the salmonella effector SPTP bound to RAC1, Mol. Cell 6 (2000) 1449–1460.

[24] N. Guex, M.C. Peitsch, SWISS-MODEL and the Swiss-Pdb-Viewer: An environment for comparative protein modeling, Electrophoresis 18 (15) (1997) 2714–2723.
[25] W.F. van Gunsteren, S.R. Billeter, A.A. Eising, P.H. Hünenberger, P. Krüger, A.E. Mark, W.R.P. Scott, I.G. Tironi, Bimolecular simulation: The GROMOS96 manual and user guide, Hochschulverlag an der ETH Zürich/Biomos, Zürich/Groningen (1996).
[26] A.J. Adler, N.J. Greenfield, G.D. Fasman, Circular dichroism and optical rotatory dispersion of proteins and polypeptides, Methods Enzymol. 27 (1973) 675–735.
[27] F.D. Sönnichsen, J.E. Van Eyk, R.S. Hodges, B.D. Sykes, Effect of trifluoroethanol on protein secondary structure: An NMR and CD study using a synthetic actin peptide, Biochemistry 31 (1992) 8790–8798.
[28] H.J. Dyson, M. Rance, R.A. Houghten, P.E. Wright, R.A. Lerner, Folding of immunogenic peptide fragments of proteins in water solution. II. The nascent helix, J. Mol. Biol. 201 (1988) 201–217.
[29] H.J. Dyson, P.E. Wright, Defining solution conformations of small linear peptides, Annu. Rev. Biophys. Biophys. Chem. 20 (1991) 519–538.
[30] S.R. Lehrman, J.L. Tuls, M. Lund, Peptide α-helicity in aqueous trifluoroethanol: Correlations with predicted α-helicity and the secondary structure of the corresponding regions of bovine growth hormone, Biochemistry 29 (1990) 5590–5596.
[31] T.J. Wallace, A. Schriesheim, W. Bartok, The base-catalyzed oxidation of mercaptans. III. Role of the solvent and effect of mercaptan structure on the rate determining step, J. Org. Chem. 26 (1963) 1311–1314.
[32] K. Wüthrich, NMR of Proteins and Nucleic Acids, Wiley-Interscience, New York, 1986.
[33] D.S. Wishart, B.D. Sykes, F.M. Richards, The chemical shift index: A fast and simple method for the assignment of protein secondary structure through NMR spectroscopy, Biochemistry 31 (1992) 1647–1651.
[34] D.S. Wishart, C.G. Bigam, A. Holm, R.S. Hodges, B.D. Sykes, ^{1}H, ^{13}C and ^{15}N random coil NMR chemical shifts of the common amino acids. I. Investigations of nearest-neighbor effects, J. Biomol. NMR 5 (1995) 67–81.
[35] T.P. Creamer, G.D. Rose, Interactions between hydrophobic side chains within α-helices, Protein Sci. 4 (1995) 1305–1314.
[36] N.D. Lazo, D.T. Downing, Stabilization of amphipathic alpha-helical and beta-helical conformations in synthetic peptides in the presence and absence of ionic interactions, J. Pept. Res. 51 (1998) 85–89.
[37] J.H. Dyson, M. Rance, R.A. Houghten, R.A. Lerner, P.E. Wright, Folding of immunogenic peptide fragments of proteins in water solution. I. Sequence requirements for the formation of a reverse turn, J. Mol. Biol. 201 (1988) 161–200.
[38] G. Merutka, H.J. Dyson, P.E. Wright, Random coil ^{1}H chemical shifts obtained as a function of temperature and trifluoroethanol concentration for the peptide series GGXGG, J. Biomol. NMR 5 (1995) 14–24.
[39] M. Cserzo, E. Wallin, I. Simon, G. von Heijne, A. Elofsson, Prediction of transmembrane alpha-helices in procaryotic membrane proteins: The Dense Alignment Surface method, Prot. Eng. 10 (1997) 673–676.
[40] M. Harada, Y. Habata, M. Hosoya, K. Nishi, R. Fujii, M. Kobayashi, S. Hinuma, N-Formylated humanin activates both formyl peptide receptor-like 1 and 2, Biochem. Biophys. Res. Commun. 324 (2004) 255–261.
[41] B. Martoglio, B. Dobberstein, Snapshots of membrane-translocating proteins, Trends Cell Biol. 8 (1998) 410–415.
[42] J. Seelig, Thermodynamics of lipid–peptide interactions, Biochim. Biophys. Acta 1666 (2004) 40–50.
[43] G. von Heijne, The signal peptide, J. Membr. Biol. 115 (1990) 195–201.